CELL BIOLOGY

Escherichia coli as a platform for the study of phosphoinositide biology

Sergio Botero*, Rachel Chiaroni-Clarke†, Sanford M. Simon‡

Despite being a minor component of cells, phosphoinositides are essential for eukaryotic membrane biology, serving as markers of organelle identity and involved in several signaling cascades. Their many functions, combined with alternative synthesis pathways, make in vivo study very difficult. In vitro studies are limited by their inability to fully recapitulate the complexities of membranes in living cells. We engineered the biosynthetic pathway for the most abundant phosphoinositides into the bacterium *Escherichia coli*, which is naturally devoid of this class of phospholipids. These modified *E. coli*, when grown in the presence of *myo*-inositol, incorporate phosphatidylinositol (PI), phosphatidylinositol-4-phosphate (PI4P), phosphatidylinositol-4,5-bisphosphate (PIP2), and phosphatidylinositol-3,4,5-trisphosphate (PIP3) into their plasma membrane. We tested models of biophysical mechanisms with these phosphoinositides in a living membrane, using our system to evaluate the role of PIP2 in nonconventional protein export of human basic fibroblast growth factor 2. We found that PI alone is sufficient for the process.

INTRODUCTION

Phosphoinositides are a class of phospholipids characterized by a six-carbon ring, *myo*-inositol head group. They are present in small quantities in all eukaryotes and some groups of bacteria and archaea (*1*). Their diversity is higher in eukaryotes, where they are phosphorylated at their third, fourth, and fifth positions of the inositol ring. This phosphorylation can occur in any combination of sites, which results in an eight-option code. Phosphoinositides with different phosphorylation states are synthesized in different membranes. In turn, proteins that have evolved to recognize specific phosphoinositides localize to the membranes enriched in the phosphorylated phosphoinositides that they recognize. The combination of specific phosphoinositides and their respective protein interactors creates a scaffold for organelle identity (*2*). Because of this, functions for phosphoinositides include a wide range of cellular processes, including cell division (*3*), actin organization (*4*), membrane curvature (*5*), ion channel activity (*6*), nonconventional protein export (*7*), chromatin maintenance (*8*), protein anchoring to the plasma membrane in the form of glycophosphoinositides (*9*), and signal transduction (*10*).

Most of the known functions of phosphoinositides come from their role as protein scaffolds (*2*). This can be through direct protein-phosphoinositide interactions or through interactions with other proteins that in turn interact with phosphoinositides, of which Rab guanosine triphosphatases are particularly relevant (*11*). Many protein domains have been identified as direct interactors with phosphoinositides, including PH (pleckstrin homology), ENTH (epsin N-terminal homology), CALM (clathrin assembly lymphoid myeloid), ANTH (AP180 N-terminal homology), PTB (phosphotyrosine binding), BAR (Bin, amphiphysin, and Rvs), PX (phox homology), postsynaptic density protein, *Drosophila* disc large tumor suppressor, PDZ (Zonula occludens–1 protein), FERM (F-actin binding ezrin, moesin, and radixin), FYVE (Fab 1, YOTB, Vac 1, and EEA), and C2 and Tubby domains (*2*, *12*, *13*), and the affinity and specificity of these vary widely, with some very promiscuous interactions driven mainly by charge (*14*). The inositol head group can also be cleaved from the rest of the phosphatidylinositol 4,5-bisphosphate (PIP2) phospholipid, generating inositol triphosphate and diacylglycerol, which are important intracellular messengers (*15*). Inositides, the phosphorylated versions of inositol, can also act as compatible solutes (*16*), cofactors for RNA and DNA regulation (*17*), and protein modification moieties (*18*).

In eukaryotic cells, phosphoinositides are synthesized in the endoplasmic reticulum (ER) initially as phosphatidylinositol (PI) from inositol and cytidine diphosphate diacylglycerol (CDP-DAG) (*19*), and from this pool of PI, all other phosphorylated forms are derived as the kinases and phosphatases that modify the inositol head group act on the phospholipid on different membranes. The specificity of these enzymes varies considerably, and there is redundancy in their function (*20*), as well as apparent distinct pools of the same phosphoinositide (*21*), although it remains unclear how these are maintained separate. Segregation across organelles (*22*) and sequestration by proteins (*23*) add another level of complexity to the regulation of phosphoinositide abundance.

The study of phosphoinositides in vivo is complicated by their involvement in a multitude of functions with alternate synthesis pathways. Thus, when a specific phosphoinositide's abundance is modified experimentally, multiple pathways are affected. Visualization studies take advantage of phosphoinositide-binding domain specificity to track their localization (*24*), but even this type of measure could potentially interfere with their functions, since there would be competition between the protein binders of interest and the reporters for the available phosphoinositides (*25*). On the other hand, in vitro studies allow good control of the components present without the potential problem of altering other functions. Unfortunately, the phospholipid membranes, vesicles, and micelles used do not fully recapitulate the very complex dynamics of membranes in living cells.

In the present study, we try to bridge the gap between in vivo and in vitro studies of phosphoinositides by creating a new bacterial tool for their study. For this, we use *Escherichia coli*, a bacterium that is naturally devoid of any phosphoinositides and lacks the metabolic ability to synthesize *myo*-inositol (*26*). In addition, being a very well characterized model organism, this bacterium maximizes the potential uses of the system we developed, since protein expression can be tightly regulated, and potential confounding factors, such as proteins homologous to those being introduced, are most likely well described. We designed a set of plasmids that allow for the expression of

Laboratory of Cellular Biophysics, Rockefeller University, New York, NY, USA.
*Present address: Stern School of Business, New York University, New York, NY, USA.
†Present address: Murdoch Children's Research Institute, Parkville, Australia.
‡Corresponding author. Email: simon@rockefeller.edu

the enzymes required for the production of the three most abundant phosphoinositides in the mammalian cell: phosphatidylinositol (PI), phosphatidylinositol-4-phosphate (PI4P), and phosphatidyl inositol 4,3 bisphosphate [PI(4,5)P_2] (or simply PIP2). Because *E. coli* does not have any proteins that should interact specifically with phosphoinositides, it is then possible to test the sufficiency of a set of components for a specific model of cell biology, without the difficulties that doing this type of test would have in a mammalian cell, in terms of altering other cellular processes and the virtual impossibility of demonstrating that there are no other endogenous factors relevant to the process being studied.

Our system also takes advantage of the lack of the inositol precursor in the cell to allow for control of phosphoinositide production by varying the presence of inositol in the growth media. We start from the previously reported synthesis of PI upon expression of a PI synthase (PIS) and the addition of inositol to the media (*27*) and build on it by producing PI4P with the addition of a PI-4-kinase (PI4K) and further phosphorylating PI4P to produce PIP2 with the addition of a PI4P-5-kinase (PI4P5K). We show that our system effectively produces the desired phosphoinositides and that the amounts can be controlled by varying the inositol in the media.

Last, to illustrate a potential use for our system, we use it to test the relevance of PIP2 for the export of human basic fibroblast growth factor 2 (FGF2). Proteins are exported from eukaryotic cells using two classes of pathways. One is a "public" pathway shared by large numbers of proteins, which requires targeting to the ER, specific machinery to cross the membrane (*28*), and further machinery to be transported through the secretory pathway (e.g., the Golgi and transport vesicles) and out of the cell. This general pathway is known as conventional protein export. The second, known as nonconventional protein export, is a "private" pathway, which seems to be specific to individual proteins and is believed to occur directly across the plasma membrane through mechanisms that are contested. FGF2 is a classic example of a protein that uses such a private pathway (*29*). The current model proposes that FGF2 is translated and released into the cytoplasm, after which it becomes phosphorylated at tyrosine 82 by Tec kinase (*30*). It is not clear whether this phosphorylation occurs in the cytoplasm or at the plasma membrane, but it is more likely that it occurs at the plasma membrane given that it is the normal Tec kinase localization (*30*). This phosphorylation enhances FGF2 oligomerization after binding to PIP2, for which it has a K_d of approximately 1 μM (*31*). PIP2 binding drives membrane localization and, together with the phosphorylation at tyrosine 82, induces oligomerization of FGF2 (*32*). While the lack of this phosphorylation diminishes export of FGF2, it does not entirely abolish it (*7*), suggesting that the system is perhaps more robust than expected. After FGF2 has oligomerized, it has been proposed that a membrane pore is produced, which allows the diffusion of small molecules and FGF2 to cross through the plasma membrane, reaching the extracellular space. This pore is hypothesized to be lined with PIP2, although this has only been shown to be the case in vitro (*7*). Unlike transport through the public systems, which requires a protein to be unfolded to transport, it has been shown that FGF2 exports in a fully folded conformation and that the folded state is required for its export (*33*).

There is evidence supporting each step of the process involved in export of FGF2. However, it has been impossible to confirm the sufficiency of the proposed components in vivo. An in vivo, independent test for the sufficiency of the proposed components would provide very strong support for the model. There are additional experimental advantages to using FGF2 export to test this system for studying phosphoinositides. First, FGF2 export is not impaired when it is fused to a protein tag, such as green fluorescent protein (GFP), and for our test, we fuse it to a small luciferase such that export of FGF2 out of the cytoplasm would increase the luminescence signal. Second, a phosphomimic using glutamate substitution for tyrosine 82 (Y82E) has been shown to completely restore FGF2 export when Tec kinase activity was experimentally ablated (*30*), providing a simple way to obviate the need for Tec kinase. Third, the binding site for PIP2 can also be eliminated by using three point mutations—K127Q, R128Q, and K133Q (*32*)—thus providing a reduced export control. Last, it has been shown that two cysteines exposed on the surface of FGF2 are important for the final steps of export (the oligomerization and formation of the hypothesized membrane pore) and that mutating them to alanine diminishes export (mutations C77A and C95A). In addition, there is a related molecule, fibroblast growth factor 4 (FGF4), that uses a signal sequence to be translocated across the ER and exported through the secretory pathway in a conventional way. When the signal sequence is deleted and mutations are made at their equivalent positions to introduce these cysteines, the binding site for PIP2, and the phosphomimic, FGF4 acquires the ability to be exported in the same way as FGF2 (*34*), thus providing us with an additional test to verify our results. The proposed PIP2-mediated export of FGF2 presents an interesting opportunity to show an application for the system we have developed.

RESULTS

Our strategy uses one of the known metabolic pathways for the production of PIP2 (Fig. 1). The expression of PIS and the ability to vary the inositol to regulate the production of PI in *E. coli* had been shown previously in the literature (*27*). We engineered a myc-tagged PIS to express PI. To phosphorylate PI into PI4P, we engineered a myc-tagged PI4K, and to phosphorylate PI4P into PIP2, we engineered an additional myc-tagged PI4P5K. The constructs for the production of only PI or PI4P differ from the one for the production of PIP2, which has all three enzymes and is shown in Fig. 1, simply in that they lack the additional enzymes required for the phosphorylation (no myc-PI4P5K for PI4P production, and no kinases for PI production).

When the synthetic enzymes were expressed using a high–copy number plasmid, a number of morphological abnormalities were observed in the bacteria (fig. S1). These abnormalities consisted of large inclusion bodies, elongated cells even in the absence of the addition of inositol when grown in LB media, and long filamentous cells in some constructs when grown with 2 mM inositol.

In contrast, when the synthetic enzymes were expressed from a low–copy number plasmid, no adverse effects were detected in the morphology of the cells or their growth rate. No effects were observed on the cells in the presence of inositol up to 10 mM (Fig. 2A). However, at concentrations of inositol above 10 mM, there was a decline in growth, and 18 mM was lethal. The adverse effect of inositol was not observed in the control lacking phosphoinositide synthesizing enzymes. The effect on growth is observed even for the strain that only had the enzyme sufficient for synthesizing PI. Thus, the lethality is likely due to the properties of PI directly, possibly its bulkier head group compared to the normal *E. coli* phospholipids, or due to the depletion of the precursor diacylglycerol. It is possible that the enhanced growth defects observed in the constructs expressing PI4P5K reflect an additional effect of the high charge of PI4P or PIP2. This lethality effect imposes a limitation of a maximum of 10 mM inositol in the

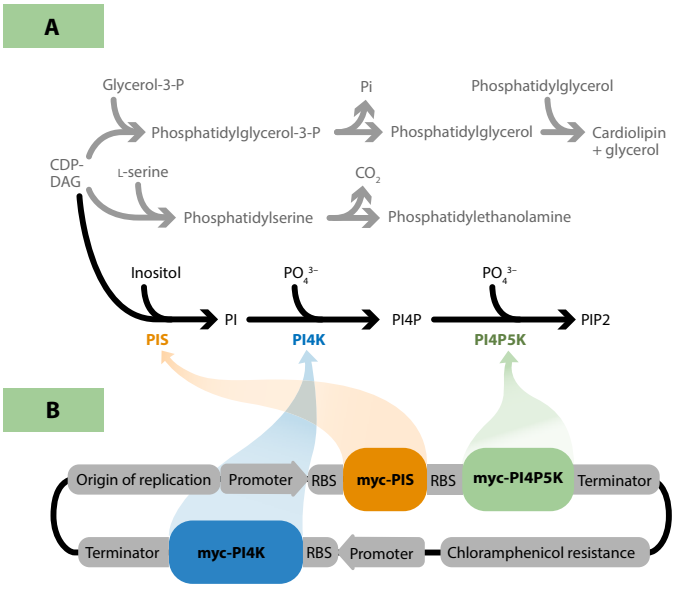

Fig. 1. Synthesis of PIP2 in bacteria. Metabolic pathway for phospholipid production in *E. coli* and construct design for the expression of the required enzymes. (**A**) *E. coli* phospholipid metabolic pathway and designed PIP2 synthesis pathway. CDP-DAG, cytidine diphosphate diacylglycerol. (**B**) Map of the construct for the expression of the enzymes required for PIP2 synthesis. RBS, ribosome binding site.

media for the conditions used in our study, and we therefore limited subsequent concentrations to 5 mM or less. We chose this low–copy number plasmid to perform the experiments we present but report the observed abnormalities with the high–copy number plasmid, as they could be relevant for researchers interested in other topics.

To detect the production of PI4P using our initial high–copy number plasmid constructs, we used a protein lipid overlay assay. These tests showed the expected production of PI4P. However, we expected that when only PIS and PI4P5K are expressed, only PI would be produced (due to the absence of PI4K), but there was also production of PI4P (fig. S2). This result is consistent with PI4P5K being promiscuous in its substrate use, being able to make PI4P from PI. The fact that PI4P is detected also indicates that this PI4P5K can phosphorylate PI in its fourth position and release it without simultaneously phosphorylating PI in its fifth position. If it were to phosphorylate both fourth and fifth positions simultaneously, only PI and PIP2 would be observed. To test the validity of these results and particularly the unexpected production of PI4P from PI by PI4P5K, we repeated the experiment with the low–copy number plasmid constructs. We quantified the production of both PI4P and PIP2 with these other constructs, but this time we used an enzyme-linked immunosorbent assay (ELISA) for improved quantification, using the values observed by mass spectrometry to perform a linear correction for systematic losses during the extraction and ELISA procedures (Fig. 2B; see below for a discussion of mass spectrometry results). Again, we observed the production of PIP2 and PI4P with the expression of PIS and PI4P5K in the absence of PI4K.

For all of these experiments, the cells are stably expressing the enzymes, and the synthesis of the phosphoinositides is initiated by the addition of inositol to the media. Thus, there should be an inherent time component to the amount of phosphoinositides in the cell. The expectation is that the relative expression of phosphoinositides to other lipids will increase over time until they reach a maximum. Then, after the remaining inositol in the media cannot provide a precursor for the new synthesis of phosphoinositides, the relative levels of phosphoinositides should decrease because of dilution by cell growth and division. A time course measure shows that both PI4P and PIP2 follow this expected behavior in cells expressing PIS, PI4K, and PI4P5K, with a maximum of phosphoinositide accumulation around 3 hours of culture (Fig. 3A).

To test the effects of different concentrations of inositol in the media, we incubated the cells expressing the biosynthetic enzymes with different levels of inositol. More PIP2 and PI4P were produced with higher levels of inositol, but the production of the phosphoinositides saturated at a concentration of approximately 2 mM inositol (Fig. 3B). Even without adding inositol, we detected a limited signal from the assay for PIP2 and PI4P (Figs. 2B and 3, A and B). One possibility was that this was the consequence of low background levels of inositol in our media acting as substrates for the enzymes. However, we do not think this is the case because the low level of signal is seen in the absence of expressing kinases PIS, PI4K, and PI4P5K in a wild-type *E. coli* background (Fig. 2B). Thus, we think that it is a background signal for the assay but not reflective of low levels of PI4P and PIP2. Since the calibration curve is not linear, we report the values as measured, instead of performing a correction by subtracting the value at 0 mM inositol.

As an independent method of quantification of changes in the phospholipids in the bacterial membrane, we used mass spectrometry. Our first assay quantified all classes of phospholipids in *E. coli*, including PI, but missed some lipid tail configurations and phosphorylated phosphoinositides. Since phosphorylated phosphoinositides could not be detected by the original assay, we only probed *E. coli* expressing PIS. We complemented this assay with a more detailed mass spectrometry measure of the phosphoinositides, including PI monophosphates (PIP) and PIP2 (see Materials and Methods). The data show that phosphatidic acid, a precursor of all phospholipids, is consumed as inositol concentration is increased. Phosphatidylglycerol is consumed proportionally faster than phosphatidylethanolamine (PE), as the concentration of inositol increases (Fig. 3C). Mass spectrometry analyses also showed a very small level of background noise for the phosphoinositides, at most 0.1% of the total phospholipids. Surprisingly, we detected the presence of phosphatidylinositol-3,4,5-trisphosphate (PIP3) when PIS, PI4K, and PI4P5K were present or when just PIS and PI4P5K were present, reaching 0.59 and 0.73% of the total phospholipids, respectively, indicating that PI4P5K can phosphorylate PI at its third, fourth, and fifth positions. To test whether it was possible to increase the amount of PIP3, we created a construct that also expressed PI-3-kinase (PI3K). When PIS, PI4P5K, and the hyperactive mutant E545K of PI3K, which is constitutively active, are expressed together, PIP3 reached 1.3% of the total phospholipids (Fig. 3C and table S1). Notably, while we assume that the totality of PIP detected should be PI4P, the analysis is unable to distinguish isoforms of this; thus, it is possible that it is a mixture of PI4P and the rarer forms PI3P and PI5P. Given the promiscuous nature of PI4P5K in our system, it would not be surprising if, in fact, the PIP detected is a mixture of all three isoforms.

We used kinase inhibitors to test for the presence of endogenous phosphatases that might be dephosphorylating the synthesized phosphoinositides. Our test showed that PI4P decreased by 58% in cells expressing PIS and PI4K when treated with PIK-93 (a PI4K inhibitor) while PI remained virtually unchanged (0.46% increase). For

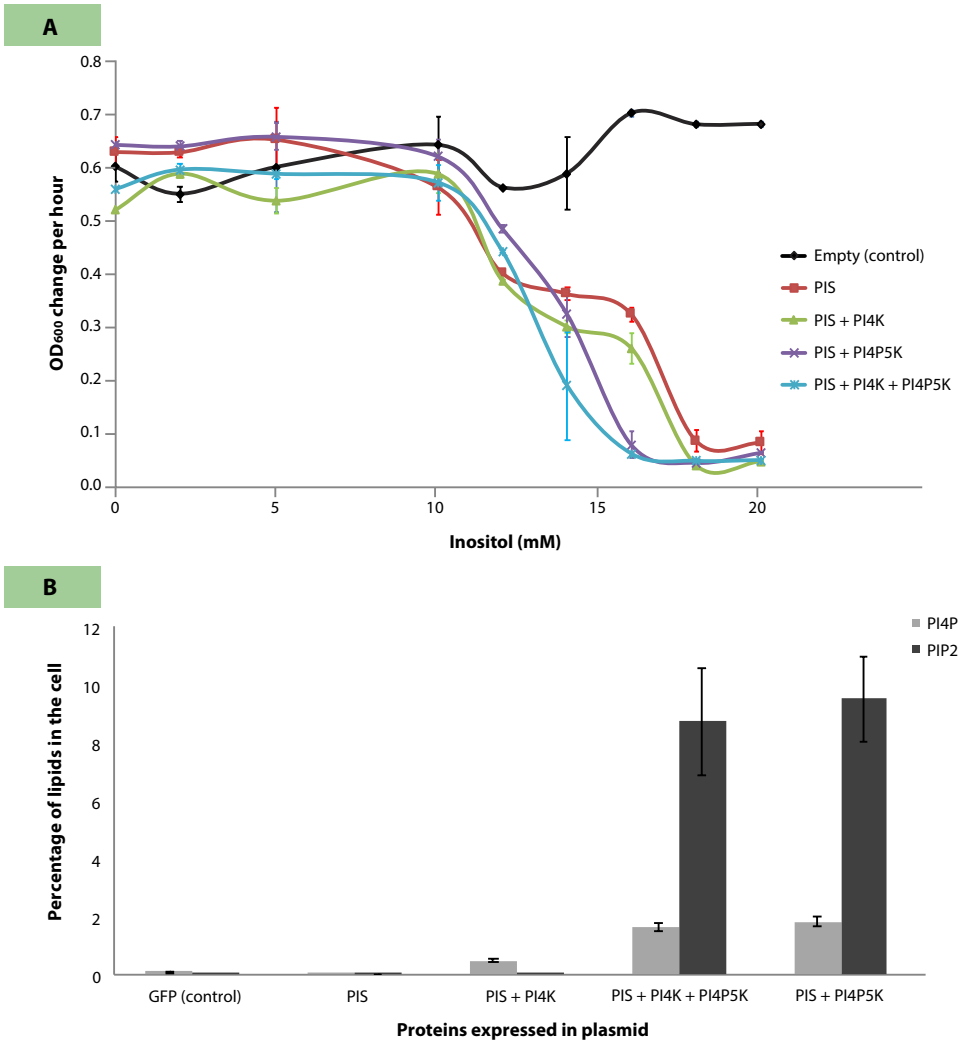

Fig. 2. *E. coli* growth during phosphoinositide production. Effect of the different constructs on *E. coli* growth and synthesis of phosphorylated phosphoinositides. (**A**) Effects of inositol on the growth rate of *E. coli* expressing the different constructs. The data presented are the maximum growth rate observed for each construct during the exponential growth phase in LB media at 37°C. Error bars show the SD of three replicates. (**B**) Production of PI4P and PIP2 for the optimized constructs reported in this study. Cells were grown for 3 hours in LB media with 2 mM inositol. Data shown are the average of four independent measures with error bars showing the SD of the sample.

cells expressing PIS, PI4K, and PI4P5K, PI4P and PIP2 decreased by 27 and 24%, respectively, when cells were treated with ISA-2011B (a PI4P5K inhibitor). In contrast, PI increased by 2% with the inhibition of PI4P5K. The decrease in the abundance of PI4P in this case is likely due to the diminished activity of the promiscuous PI4P5K, which can phosphorylate both sites (fourth and fifth positions), rather than the inhibition of PI4K. These results reflect some level of endogenous phosphatase activity in the bacterial cell that it is more relevant for PI4P than for PIP2, suggesting this to be a potential cause for the relatively lower levels of PI4P than PIP2 produced.

There are some trends in the lipid tails in the *E. coli* producing phosphoinositides relative to those of wild-type *E. coli* (table S1). The C32:1 and C34:1 lipid configurations, which are the most common configuration of *E. coli*'s PE (*35*), are also the most common configuration observed in the phosphoinositides. This suggests that there is little selectivity in the choice of lipids by the enzymes. Despite this, PE 34:2, the fourth most abundant PE, falls more drastically than PE 32:0, the third most abundant PE, as phosphoinositides are produced, suggesting some level of preference by the PIS for the 34:2 over the 32:0 configuration.

As an independent way to show that our system produces phosphorylated phosphoinositides, we attempted another type of assay based on the binding of proteins to phosphoinositides. For this assay, a GFP reporter is fused to protein domains that recognize either PI4P [OSBP-PH domain (PH domain of oxysterol-binding protein) and SidM-P4M domain] (*36*, *37*) or PIP2 [PH domain of phospholipase Cδ1 (PLCδ-PH domain)] (*38*) and is expressed in *E. coli*. When phosphoinositides are present, the fluorescence should localize to the plasma membrane because of the recognition of the phospholipid by the protein reporters, creating a "halo" when visualized under the microscope. The same cells can be grown in media without inositol to have a negative control to show that the localization of the reporter is not caused by an unexpected interaction with other components of the cell or with the proteins that our system expresses to produce the

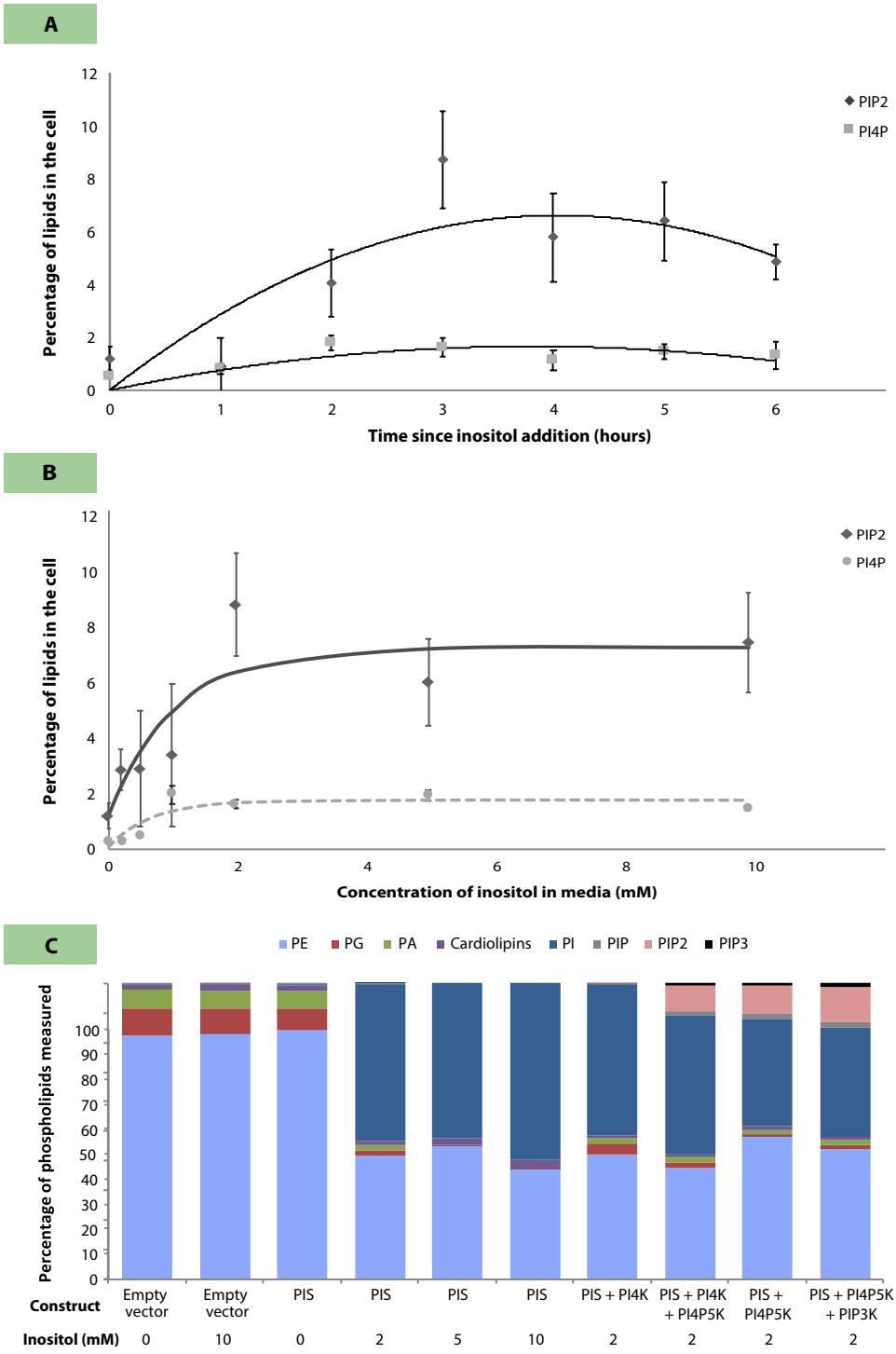

Fig. 3. Phosphoinositides and phospholipids in *E. coli*. Characterization of the changes in phosphoinositides and overall phospholipids produced in *E. coli*. (**A**) Time course of phosphorylated phosphoinositide production. Cells expressing the enzymes PIS, PI4K, and PI4P5K were assayed for PIP2 and PI4P after the addition of 2 mM inositol. The amount of culture pelleted was adjusted to obtain a pellet equivalent to 10 ml of culture at an optical density at 600 nm (OD_{600}) = 1 for lipid extraction. Trend curves are from a second-order polynomial. Data shown are the average of four independent measures with error bars showing the SD of the sample. **(B)** Phosphoinositide production under different inositol concentrations. Cells expressing the biosynthetic enzymes PIS, PI4K, and PI4P5K were supplemented with varying concentrations of inositol. At 3 hours, the cell concentration was adjusted to obtain a pellet equivalent to 10 ml of culture at OD_{600} = 1 for lipid extraction. Trend curves are from an exponential fit of the form $y = a + be^{(-cx)}$. Data shown are the average of four independent measures with error bars showing the SD of the sample. (**C**) Change in the abundance of major phospholipid categories in *E. coli* upon production of phosphoinositides. The percentage of each phospholipid group is illustrated. For this experiment, cells were grown in LB media supplemented with different concentrations of inositol. PA, phosphatidic acid; PG, phosphatidyl glycerol; PE, phosphatidyl ethanolamine.

phosphoinositides. The fluorescence should then be diffuse in the cytoplasm when inositol is not added to the media. As an internal control, we also expressed a red fluorescent protein, mCherry, so that the cytoplasm volume could be easily visualized in the red channel, while the reporter is visualized in the green channel. An example of positive and negative localization of the probes is shown in Fig. 4A.

To probe for the presence of PI4P, we used the P4M domain of the SidM protein from *Legionella pneumophila*, which has been previously used as a tandem 2 copy construct fused to GFP to detect PI4P (*37*). These tests showed the expected localization of PI4P in the plasma membrane of the bacterium (Fig. 4B). As a parallel test, we used the PI4P-binding OSBP-PH domain, which failed to reveal membrane localization. It is possible that this was due to a technical problem: The SidM is a bacterial protein and the OSBP is eukaryotic and may not have folded properly in *E. coli*. Alternatively, the SidM is a tandem construct and can detect lower levels of PI4P. Since we found the correct localization of the P4M probe and other independent lines of evidence for the detection of PI4P, we performed no further tests using the PI4P-binding OSBP-PH reporter. The detection of PIP2 with the PLCδ-PH domain proved successful, showing the expected halo (Fig. 4C).

To test for the localization of phosphoinositides, we collected fluorescence images of the GFP-tagged phosphoinositide-binding domain and of cytosolic mCherry. The distribution of the phosphoinositide-binding reporter relative to the cytosolic marker was probed with a line plot across the center of the cell. If the reporter was bound to the plasma membrane, then the distribution across the cell should be bimodal, and if the reporter was cytosolic, then it should have a unimodal distribution (see Materials and Methods). An index was established, which has a value of 1 for perfectly unimodal distributions (indicating cytoplasmic localization of the probe) or a value higher than 1 for bimodal distributions (indicating membrane localization). Since it is expected that the halo can only be visualized in cells having the enzymes required for the phosphoinositide production when grown in media containing inositol, two negative controls can be performed: cells that have the enzymes to make the phosphoinositide but are grown in media that lack inositol and cells that are grown in media with inositol but lack the enzymes required for phosphoinositide production.

As an independent third control, we used the structural knowledge of the binding of the PLCδ-PH domain to PIP2 to create a mutant that could not bind PIP2 and therefore should not localize to the membrane even when PIP2 is present. Since binding has been associated with eight specific amino acid residues (*39*), we performed nonsynonymous mutations, substituting them for alanine, such that the interaction would be impaired. The results of the fluorescent reporter analysis show that PIP2 is present in the plasma membrane only in the presence of both inositol and the phosphoinositide synthesizing enzymes and that this pattern disappears when the PLCδ-PH domain is mutated (Fig. 4C).

It has been proposed that the presence of PIP2 in the plasma membrane is necessary for export of FGF2 from mammalian cells (*32*). We tested whether our system for producing PIP2 in bacteria was sufficient for export of FGF2. To probe for a signal for export of FGF2, we tagged it with a small luciferase (nanoLuc). We performed tests on a set of three constructs: (i) a minimum export mutant that has both cysteines involved in export mutated to alanine and has a mutant binding site for PIP2 and thus also having impaired binding, (ii) a wild-type protein as an expected medium level of export, and (iii) a maximum export mutant that has the phosphomimic mutation Y82E in FGF2 that increases export in mammalian cells.

In this test, we expect a signal above background, measured as photon emission, only when FGF2 exports successfully out of the cytoplasm, having access to the periplasm and thus allowing the interaction of the luciferase with the membrane insoluble substrate. Since successful export of FGF2 would require not only the right FGF2 construct but also the presence of PIP2, this signal would then only be observed when inositol is added to the media. A first control was expression of mCherry fused to luciferase instead of FGF2. This evaluates whether any potential signal can be attributed to a nonspecific increase in membrane permeability due to the phosphoinositide production. A second control was the use of cells that lacked the enzymes for PIP2 synthesis to verify that the effect was not simply due to inositol in the media. The export of the reporter luciferase out of the *E. coli* expressing the phosphoinositide synthesizing enzymes was assayed in the presence of different concentrations of inositol.

For cells expressing each of the FGF2 constructs, a luciferase signal that increased in magnitude with increasing addition of inositol was detected. This inositol-dependent signal was only observed when the PIP2 synthesizing enzymes were present. This is consistent with the hypothesis that an inositol-dependent production of PIP2 by the phosphoinositide kinases was responsible for the export of FGF2. For the control construct of nanoLuc fused to mCherry, there was no increased signal in response to the addition of inositol or any difference due to the presence or absence of the inositol kinases. This confirms that the effects observed are in fact due to the export of FGF2 from the cell (Fig. 5A). The wild-type and phosphomimic constructs showed similar increases in signal upon inositol addition, and the minimal export construct, which has impaired PIP2 binding and lacks the cysteines involved in oligomerization, also showed export dependent on the presence of PIP2, albeit lower than that of the wild-type and phosphomimic constructs. This observation is surprising since, based on the current model, we expected the minimal export construct to show only baseline levels of export and the phosphomimic construct to export The specificity of these enzymes varies considerably more than the wild type. Initially, we had included all possible constructs to account for all combinations of mutations proposed as relevant to the export process (no PIP2 binding, no cysteines, and phosphomimic), but the results were not clear in terms of the relationship of the current functional model and the mutations (see fig. S5).

FGF4 is similar in structure to FGF2 but has an N-terminal signal sequence that targets it for entry into the secretory pathway of eukaryotic cells at the ER and is exported by conventional protein secretion. However, FGF4 can be induced to export in the same way as FGF2 if it is mutated to include the Tec kinase site phosphomimic, the PIP2-binding site, and the two cysteines involved in oligomerization (*34*). We refer to this construct carrying all mutations as FGF4 exporter. None of the constructs of FGF4 used for our study included the signal sequence, since it drives conventional protein export and could be a confounding factor. Thus, when we refer to a wild-type construct, it has the wild-type amino acid sequence of FGF4 but lacks the N-terminal signal sequence.

Both FGF4 wild type and FGF4 exporter showed export that depended on the addition of inositol. This was not observed in the absence of the PIP2 synthesizing enzymes (Fig. 5B). There was no increase of luciferase signal with the mCherry-luciferase, demonstrating that the effect was not the result of a nonspecific increase of membrane permeability. In all constructs, there was a low signal in the absence of

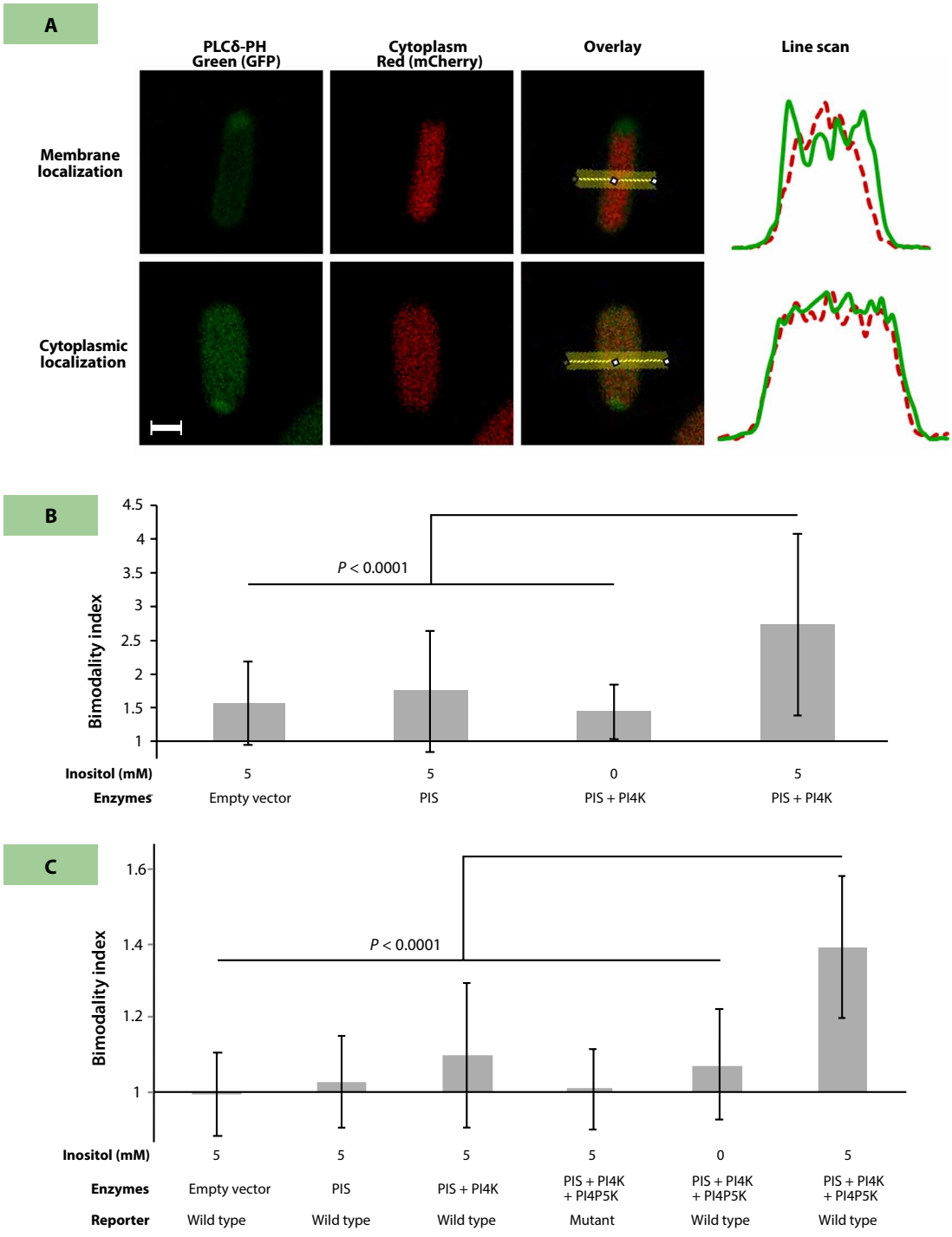

Fig. 4. PI4P and PIP2 localization. Localization of the PI4P- and PIP2-binding domains. The subcellular distribution of PI4P as assayed by the GFP-tagged SidM-P4M domain and of PIP2 as assayed by the GFP-tagged PLCδ-PH domain relative to cytosolic mCherry. (**A**) Line scans were 10 pixels wide (566 nm) and are indicated by the yellow line on the overlay image. Data from the line scans were standardized to show the same amplitude on all channels. Note the aggregation of protein toward the pole in some cells, in a way that excludes the cytoplasmic red marker, suggesting the formation of inclusion bodies even at the low level of expression used. Scale bar, 2 μm. (**B**) Subcellular distribution was quantified with a bimodality index analysis (see Materials and Methods) for the localization of PI4P in 40 cells for each construct. A one-way analysis of variance (ANOVA) indicated that treatments were different with $P < 0.0001$, and a Tukey honest significant difference (HSD) test showed that this is due to the construct where the PI4P-synthesizing enzymes are used in the presence of inositol as indicated in the figure. Error bars show the SD of the sample. An individual representative image for each treatment is provided in fig. S4A. (**C**) Subcellular distribution was quantified with a bimodality index analysis (see Materials and Methods) for the localization of PIP2 in 40 cells for each construct. A one-way ANOVA indicated that treatments were different with $P < 0.0001$, and a Tukey HSD test showed that this is due to the construct where the PIP2 synthesizing enzymes and the wild-type reporter are used in the presence of inositol as indicated in the figure. Error bars show the SD of the sample. An individual representative image for each treatment is provided in fig. S4B.

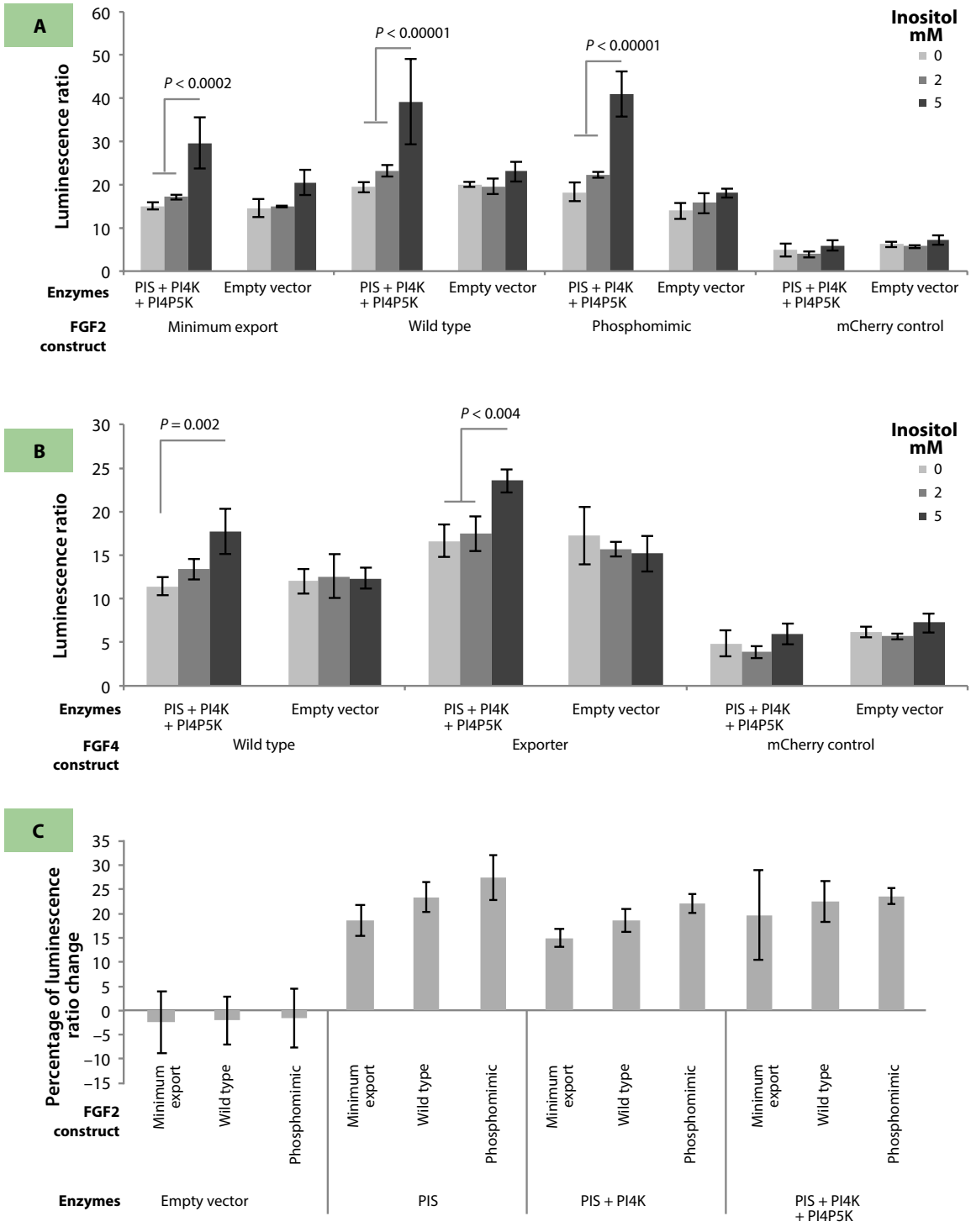

Fig. 5. Export of FGF2 and FGF4. Tests for the export of FGF2 and FGF4. (**A**) Results for FGF2 export with PIP2. A three-way ANOVA shows that each factor (presence of phosphoinositide synthesizing enzymes, amount of inositol, and FGF2 construct) is significant with $P < 0.05$ and that the interactions of inositol × synthesizing enzymes and FGF2 construct × synthesizing enzymes are also significant. Data shown are the average and SD of the sample ($n = 4$). Results of a Tukey HSD for comparison of the samples are indicated in the figure. The mCherry results were excluded from the ANOVA to avoid artificially raising the relevance of the construct for the results. (**B**) Results for FGF4 export with PIP2. A three-way ANOVA shows that each factor (presence of phosphoinositide synthesizing enzymes, amount of inositol, and FGF4 construct) is significant with $P < 0.05$ and that the interaction of inositol × synthesizing enzymes is also significant. Data shown are the average and SD of the sample ($n = 4$). Results of a Tukey HSD for comparison of the samples are indicated in the figure. The mCherry results were excluded from the ANOVA to avoid artificially raising the relevance of the construct for the results. (**C**) Export change in luminescence index of FGF2 constructs depending on the phosphoinositides present. The comparison was performed as an independent experiment comparing export with no inositol or 5 mM inositol in the media. Data shown are the average and SD of the sample ($n = 3$). Raw data are shown in fig. S6.

inositol. We assume that this is a background signal for the assay. This background varied between the constructs, although the differences were small compared to the much greater change of signal observed in the presence of inositol or inositol kinases. The variability in this "background signal" is likely due to minor differences in the stability or solubility of the different mutants used.

In a three-way analysis of variance (ANOVA), there is a significant effect of all three factors: presence of phosphoinositide synthesizing enzymes, amount of inositol, and FGF2/4 construct (the analysis was performed independently for FGF2 and FGF4). This is expected since differences among all factors should exist given the bacteria are in a different metabolic situation under each condition. Surprisingly, the interaction between the construct used and the presence of phosphoinositide synthesizing enzymes was also significant, potentially indicating some level of metabolic load due to the expression of four exogenous proteins, with variation depending on the mutant expressed. Last, the expected interaction between inositol and presence of phosphoinositide synthesizing enzymes was significant, as evaluated by a Tukey honest significant difference (HSD), indicating that, indeed, the presence of PIP2 has an effect on the signal.

While these results indicate that PIP2 is in effect stimulating FGF2 and FGF4 export, there is a background export observed for all constructs even in the absence of phosphoinositides. This suggests the possibility that phospholipids such as PE and the anionic phosphatidylglycerol present in *E. coli* are sufficient to facilitate some export of FGF2, thus the high basal background observed for these constructs compared to the mCherry control. This could also mean that the increased export observed upon inositol addition could be caused by the PI present in the cells rather than PIP2. We tested this possibility using all three constructs of FGF2 (minimal export, wild type, and phosphomimic) in combination with plasmids to evaluate whether PIP2 was necessary or PI was sufficient to generate the changes in export observed (Fig. 5C). The results of this experiment show that, in fact, PI alone is sufficient to generate the change in export observed upon the addition of inositol to the growth media at a level that is comparable to that when PI4P or both PI4P and PIP2 are present.

DISCUSSION

In the present work, we have generated a plasmid that carries all the enzymes necessary for *E. coli* to synthesize PI, PI4P, and PIP2 upon the addition of inositol to the growth media. This creates a tool that bridges the in vitro control over system components with the in vivo complexities of a living membrane when studying biophysical processes involving phosphoinositides. The use of the p15A origin of replication in our plasmids is a useful design aspect because it is a relatively uncommon origin of replication, making the plasmid compatible with most commonly used systems for bacterial protein expression and preventing plasmid loss due to incompatibility between the origins of replication used for the phosphoinositide production system and the system for production of other proteins of interest (*40*). In addition, the system that we report here can be used in virtually any *E. coli* strain since the enzymes will be expressed constitutively under the promoter proD using the endogenous RNA polymerases of the bacterium, thus not requiring the presence of T7 polymerase (*41*). A caveat to our system is that it is not clear how inositol enters the cell. The permeability of the membrane to inositol should be comparable to that of a sugar given its chemical structure, and thus, inositol does not readily cross the membrane. Since the addition of inositol to the media had previously been shown to be effective for PI synthesis (*27*), and here we show that the concentration of inositol in the media can be varied to effectively control the levels of phosphoinositide produced, how inositol crosses the membrane is of little relevance for the use of the tool we have developed. However, we caution potential users about the importance of verifying that their experimental conditions do not impede inositol uptake (i.e., test that phosphoinositides are being produced).

When characterizing our system, we observed that PIS and PI4P5K alone can produce PI, PI4P, PIP2, and even a small amount of PIP3. This is an unexpected result that suggests that PI4P5K can phosphorylate PIS at the third, fourth, and fifth positions. However, on the basis of our results, it is premature to speculate whether this occurs in the normal physiological context of the eukaryotic cell or whether there is biological significance to this observation. Since the system lacks the normal regulators of activity for this enzyme and there is no spatial segregation by an endomembranous system, this activity might be irrelevant in vivo. However, while we still used the system expressing all three enzymes for our tests to be conservative, this observation opens the possibility of using the system with just PIS and PI4P5K when PIP2 production is desired to reduce the metabolic load of the expression of PI4K, which is apparently unnecessary. It also opens the possibility of enhancing the production of PIP3, by expressing PIS, PI4P5K, and PI3K simultaneously, and we have shown that this approach can produce PIP3 up to 1.3% of the total phospholipids.

The morphological abnormalities observed when using high–copy number plasmids for the expression of the phosphoinositide synthesizing enzymes (fig. S1) and the lethality of high concentrations of inositol in the growth media when phosphoinositide synthesizing enzymes are present are not unexpected. Long *E. coli* cells have been observed when phosphatidylserine synthetase is defective, leading to a decrease in PE (phosphatidyl serine is a precursor to PE) and an increase in cardiolipins and phosphatidylglycerol (PG). This mutation has been reported to induce the formation of very elongated cells that elongate until death occurs (*42*). PI replacing PG is also lethal (*43*); thus, it is likely that the observed defects when using the very high expression constructs and the growth defects under concentration of inositol in the media higher than 10 mM simply reflect a phenotype product of the simultaneous decrease of PG and PE.

The characterization of our system shows a time-dependent component to phosphoinositide accumulation levels in a batch culture system (Fig. 3A) and the ability to control the levels of phosphoinositide produced by varying the levels of inositol in the media (Fig. 3B). The apparent plateau for maximum quantities of phosphoinositides observed when varying the inositol concentration is possibly due to some level of autoinhibition by the kinases upon an increase in their product. The autoinhibition of PI4K can be inferred from analyzing the results of phosphoinositide production when expressing different sets of enzymes (Fig. 2B). In particular, when PIS and PI4K are expressed simultaneously, about 0.5% of the lipids in the cell are detected to be PI4P, but when all three enzymes are expressed, 1.6% is PI4P and 8.7% is PIP2, adding up to 10.3%. Since all PIP2 in the process of biosynthesis goes through an intermediary of PI4P, this suggests that the cells produced more than twice as much PI4P when PI4P5K was present than when it was absent. This suggests that the phosphorylation of PI4P into PIP2 releases some of the autoinhibition of PI4K. The fact that the levels of phosphorylated phosphoinositides are very similar when all three enzymes are present or when only PIS and PI4P5K

are expressed also indicates autoinhibition of PI4K by its product or an even larger amount of PI4P should be detected. Given that the amount of PIP2 produced is small compared to the amount of PI that can be generated, it is likely that PI4P5K also shows some level of autoinhibition, but we lack direct evidence of this phenomenon. Our test with kinase inhibitors shows that there are endogenous phosphatases in the cell, and this is an additional factor limiting the amounts of phosphorylated phosphoinositides produced. For tests in which the goal is to observe an increase (or decrease) in the reporter signal measured as more phosphoinositides are produced because of the addition of more inositol, the autoinhibition of the kinases and the presence of phosphatases are not a problem; the signal will show a monotonic trend regardless of the feedback loop, allowing the desired comparisons to be made. However, albeit monotonic, the feedback loop will cause the response to be nonlinear, and caution must be exercised to work on a range of inositol relevant for the experiment at hand. For researchers interested in using our system for applications where the absolute availability of phosphoinositides needs to be controlled, this feedback loop might be a more serious consideration, and care should be exercised to characterize the system in detail under the specific culture conditions relevant to such experiments.

An important aspect of this system is the level of phosphoinositides reached relative to those in eukaryotic cells. We report the levels of phosphoinositide production in our system as a percentage of the total lipids by mass to allow a direct comparison to the levels of phosphoinositides in eukaryotic cells. The range observed, around 2 and 12% maximum for PI4P and PIP2, respectively (Fig. 3A), is up to an order of magnitude higher than the range observed in mammalian cells, in which PI4P and PIP2 each represents about 0.5 to 1% of the total phospholipids (*44*). Considering that, in eukaryotic cells, phosphoinositides interact with a wide variety of proteins at all times and might be segregated in several membranes, the amount of free phosphoinositides in these cells should be significantly lower than the 0.5% value; thus, the amount produced by the system presented here should allow one to test most cell biology models of interest with levels of available phosphoinositides that are equal to or higher than those in eukaryotic cells. It is possible that using the mass spectrometry data to perform a linear correction of the data measured by ELISA adds a level of error. However, the range of the estimates should be accurate given that the standards were added before the extraction for the mass spectrometry, allowing for absolute quantification, and that the values detected are close to or at the maximum for the extrapolated ELISAs. To be conservative, we warn potential users of our system that, if the precise amount of phosphoinositides is relevant for an experiment, it should be measured directly under the specific experimental conditions of interest.

A major limitation to consider when using the system that we developed comes from the difference in the lipid tails present in the synthesized phosphoinositides when compared to naturally occurring eukaryotic ones. In mammals, the diacylglycerol component of phosphoinositides has between 34 and 40 C atoms, up to six double bonds, and there is always at least one double bond in one of the two lipid tails (*44*). Thus, the lipid tails present in our system will in fact be shorter than those in most eukaryotic organisms, as *E. coli* phospholipids have generally shorter and more saturated lipid tails (*35*). This difference affects membrane thickness, with a thinner membrane in *E. coli* than in most eukaryotic cells. As a result, the applicability of our system may be limited to those processes for which the main factor of interest is the head group of the phosphorylated phosphoinositide.

Our tests support a model in which phosphoinositides facilitate the export of FGF2. Surprisingly, this effect is observed even when only PI is produced. Further, there was no significant increase of export with the additional production of PI4P or PIP2 in addition to PI. This suggests that perhaps any phosphoinositide can suffice for export of FGF2 in the conditions of the *E. coli* plasma membrane.

Our results bring up two additional confounding factors. First, even when no phosphoinositides are present, both FGF2-nanoLuc and FGF4-nanoLuc have a relatively high level of export when compared to the control expression of mCherry-nanoLuc. This is not due to the absolute levels of protein expression: The mCherry construct shows much higher expression, with about one order of magnitude greater absolute luminescence signal being produced. This suggests that the FGF2 fold has a strong tendency toward export in the presence of phospholipids such as the PE and the PG present in *E. coli*'s membrane, with the anionic nature of PG possibly playing a role. This was true of the wild-type FGF2 and FGF4 or with any of the mutations of these constructs we evaluated. Second, the mutations that have been proposed in the literature as relevant for export of FGF2 do not have a discernible effect according to their proposed function. It is possible that the mutations we made on FGF2 for the PIP2-binding site might not fully eliminate binding. Clusters of basic and aromatic residues are common among domains that bind to phosphoinositides (*45*), and the site might be more general than specific to just three amino acids. Thus, the mutations to reduce the binding may have only a small effect. However, the combined lack of the phosphomimic mutation and the two cysteines proposed to be necessary for oligomerization should significantly decrease export in our minimum export construct, and only a mild effect was observed (see Fig. 5). This decrease, but not elimination of export, suggests that the protein has an intrinsic ability to export even in the absence of PIP2: The phosphorylation or oligomerization enhances an existing export phenotype. This is consistent with the basal levels of export when no inositol is added to the media. Therefore, while our results support the role of phosphoinositides in enhancing FGF2's nonconventional protein export, the FGF2 protein fold seems to have robust export abilities that seem to go beyond the currently proposed model and might be more generalized to anionic phospholipids. One caveat of our system is that the fatty acids are different; the differences in the membrane thickness and composition in *E. coli* (except for phosphoinositides) could be the cause of the differences from the observations in mammalian cells. Thus, being conservative, our results should only be taken as evidence for the enhancement of FGF2's nonconventional protein export by phosphoinositides. It is likely, as it occurs in many phosphoinositide-interacting proteins, that FGF2 has indeed a strong preference for PIP2 binding in mammalian cells over other phosphoinositides, but our results suggest an interesting possibility that merits further investigation.

One potential limitation of our system is that only positive results have relevance because a negative result might be due to many possible exogenous mechanisms, such as incorrect folding of the proteins of interest when expressed in *E. coli* or unexpected interference by a nonspecific interactor coming from the bacterium. In addition, positive results only test for the sufficiency of a set of components for a particular process; the fact that the process occurs as a model predicted does not in itself mean that the process occurs as such in living eukaryotic cells; hence, results obtained with our system for sufficiency need to be complemented with other in vivo tests to prove necessity.

In conclusion, we have developed and characterized a plasmid system for the production of phosphoinositides in *E. coli*, including PIP, PIP2, and PIP3, in which the amount of inositol added to the media can be used as a way of controlling the amount of phosphoinositides produced. While our system has some limitations, the biggest one being the fact that the lipid tails and overall membrane thickness will be different to that of eukaryotes, it provides a unique bridge between in vitro and in vivo tests by allowing researchers to test specific biophysical models of cell processes in a complex living organism but without the possibility of other related processes interfering. We have used our system to show the unexpected result that PI is sufficient to enhance the nonconventional protein export of FGF2, thus providing an example of one of the many possible applications of our system.

MATERIALS AND METHODS

Study design

The first part of the study tests the basic hypothesis that phosphorylated phosphoinositides can be produced in *E. coli*. In this way, the initial part of the report is based on a binary outcome, and while we quantify several aspects, this part of the study does not attempt to answer any further questions. To illustrate the potential for control of the system, we measured phosphoinositide production as a function of time and concentration of precursor. We also confirmed localization of PIP2 and performed an incipient characterization of the lipid substituents in the phosphoinositides produced. To get accurate and reliable estimates for our measures, we performed all experiments in triplicate except when indicated otherwise. Notably, the system we report here should work in any *E. coli* strain, but the actual levels of phosphoinositide production are expected to vary with both strain and culture conditions. Thus, the quantification that we provide is a guideline for the specific conditions we report, intended simply to show the potential control that can be obtained with our system.

The second part of the study tests the hypothesis that FGF2 export would be enhanced when PIP2 is present. We expected this to have a large effect size, and thus, we performed the experiments with relatively small sample sizes, three or four wells per treatment, depending on the experiment. We performed these tests by using nanoLuc as a reporter of protein export because the signal should be enhanced upon translocation of the reporter from the cytoplasm to the outside of the plasma membrane of the bacterium.

While the experimenter was not blinded to the nature of each sample when performing the readings, all culture tubes were labeled with codes in such a way that it was not obvious what the treatment was. In this manner, the experimenter should be unable to introduce unconscious bias in the treatment of the samples beyond pipetting error during the readouts. In the case of the fluorescence analysis, the experimenter was blinded to the results by selecting cells in the bright-field or internal control image and was, thus, unbiased to the results of the experiment.

Plasmid design, assembly, and verification

Plasmids used in this study, along with their sequence data, have been deposited in Addgene (listed in Table 1). All plasmid constructs were designed computationally and assembled using a combination of artificial synthesis of DNA, assembly polymerase chain reaction (PCR), and traditional restriction enzyme digestion followed by ligation. Restriction enzymes and the Quick Ligation Kit were acquired from New England BioLabs and used according to their recommended protocol. PCRs were performed using the Platinum PCR SuperMix or the AccuPrime Pfx SuperMix (when blunt ends were required) supplied by Thermo Fisher Scientific following their recommended protocol. Primers were designed manually and ordered from Integrated DNA Technologies. Artificially synthesized DNA was obtained from GENEWIZ. When necessary, the constructs were edited using the QuikChange Lightning Site-Directed Mutagenesis Kit from Agilent Technologies according to the manufacturer's protocol. DNA, agarose gel, and plasmid purification steps were performed using the DNA Clean & Concentrator-5 Kit, the Zymoclean Gel DNA Recovery Kit, and the Zyppy Plasmid Miniprep Kit, respectively, all obtained from Zymo Research. Visualization of agarose gels was performed using the SafeGreen Loading Dye from GeneCopoeia and visualized on a blue light-emitting diode transilluminator from IO Rodeo. All inserts were fully verified using GENEWIZ Sanger sequencing services.

The final plasmid backbones used in this study were designed in our laboratory. For the expression of the enzymes required for phosphoinositide synthesis, we initially used a modified version of plasmid pUC57-amp obtained from GENEWIZ, modifying it to have a chloramphenicol resistance marker instead of ampicillin and the T7 promoter primer and T7 terminator sequences from plasmid pET151 from Invitrogen. This plasmid has a very high copy number pUC (pMB1 derivative) family origin of replication and a T7 forward sequencing primer followed by an artificially designed constitutive promoter reported in the literature. We named this promoter simply proD to follow the nomenclature used in the original publication (*41*). However, these plasmids produced abnormal morphology of the bacterial cells in some of the constructs (see Results), limiting the potential uses for the system. Upon checking the design, this is likely due to both the very high copy number expected for a pUC plasmid and the fact that most of the sequence of the T7 promoter is in the T7 forward sequencing primer sequence. Thus, it is likely that we were getting expression from this promoter as well. We therefore discarded that initial approach and designed a lower–copy number backbone using the P15A origin of replication, which was obtained from the plasmid carried by *E. coli* BL21 DE3 from Agilent Technologies. This strain was not used in the present study, and only the origin of replication and the sequence coding for chloramphenicol resistance obtained from the plasmid it carries were used. This origin of replication was assembled into a new backbone expressing a chloramphenicol resistance marker, and the enzymes of interest under the same artificially designed constitutive promoter reported proD.

For the tests that required expression of other proteins (such as localization reporters or FGF2), we followed the same approach, designing a plasmid with a constitutive promoter, in this case using a CloDF13 origin of replication, with an ampicillin resistance marker and the same promoter proD. The CloDF13 origin of replication was obtained from plasmid pCDFDuet-1 MKK4(EE)-MKK7a1(EE) (*46*) purchased from Addgene (plasmid #47580). Only the origin of replication was used from this plasmid.

The endogenous *E. coli* terminator sequence GTTAATAACAGGCCTGCTGGTAATCGCAGGCCTTTTTATTTTTTT that comes from a replicative DNA helicase was used as a terminator sequence after all protein coding regions in the plasmids built. When two proteins needed to be expressed, we modified the backbones to have two promoters proD, oriented in the same direction but separated in one direction by the origin of replication and in the other by the

Table 1. Plasmids used in this study. All plasmids, as well as their complete sequences, are available through Addgene under the numbers indicated in the last column.

Plasmid name	Promoter used	Proteins expressed	Addgene
Plasmid type 1: Origin of replication P15A, 10 to 12 copies per cell, chloramphenicol resistance			
p15aC-GFP	proD	myc-GFP (control)	107862
p15aC-1D	proD	myc-PIS	107863
p15aC-4D1D	Dual proD	myc-PIS and myc-PI4K	107864
p15aC-1D-5	proD	myc-PIS-RBS-myc-PI4P5K (as operon)	107865
p15aC-4D1D-5	Dual proD	myc-PIS-RBS-myc-PI4P5K (as operon) and myc-PI4K	107866
p15aC-3D1D-5	Dual proD	myc-PIS-RBS-myc-PI4P5K (as operon) and PI3K	121050
Plasmid type 2: Origin of replication CloDF13, 20 to 40 copies per cell, ampicillin resistance			
pClodAcytCh-PIP2PHGFP	Dual proD	mCherry and GFP-PLCδ-PH domain	107867
pClodAcytCh-PIP2PHGFP-nb	Dual proD	mCherry and GFP-PLCδ-PH domain nonbinding mutant	107868
pClodAcytCh-GFP-P4M	Dual proD	mCherry and GFP-(2×)SidM-P4M domain	113346
pClodANL-Cherry	proD	mCherry-nanoLuc	107870
pClodANL-FGF2	proD	FGF2wt-nanoLuc	107871
pClodANL-FGF2YE	proD	FGF2phosphomimic-nanoLuc	107872
pClodANL-FGF2NBAA	proD	FGF2minimum export-nanoLuc	107873
pClodANL-FGF4	proD	FGF4wt-nanoLuc	107874
pClodANL-FGF4exporter	proD	FGF4exporter-nanoLuc	107875
Plasmid type 3: Origin of replication pUC, ~500 copies per cell, ampicillin resistance (used during optimization)			
pC51	T7-proD	myc-PI4P5K-RBS-myc-PIS (as operon)	107869

antibiotic resistance marker. In this way, if the repeated promoter leads to recombination, then the resulting plasmids will lack the antibiotic resistance or the origin of replication and thus will be eliminated. Reported copy numbers for the different origins of replication used are 10 to 12 copies per cell for P15A, 20 to 40 copies per cell for CloDF13, and approximately 500 for pUC, which is from the ColE1 family (*40*).

The enzymes for phosphoinositide production were chosen because they had been successfully produced in *E. coli* before and shown to be active when purified. *Trypanosoma brucei* PIS (*27*) was provided by T. K. Smith of the University of St Andrews (United Kingdom). Human PI4P5K type-1α isoform 2 (PI4P5Kα or PI4P5K) (*47*) was provided by R. A. Anderson of the University of Wisconsin–Madison. *Bos taurus* PI 4-kinase β (PI4Kβ or PI4K) (*48*) was provided by T. Balla of the Program for Developmental Neuroscience at the National Institutes of Health, who also provided us with the OSBP-PH domain that binds PI4P (*36*), the PLCδ-PH domain that binds PIP2 (*38*), and the GFP-P4M-SidMx2 containing plasmid as a reporter for PI4P localization (*37*). We obtained this last plasmid through Addgene (plasmid #51472), as well as the plasmid carrying a constitutively active E545K mutant of human PI3K catalytic subunit p110α of class IA (PI3K) (plasmid #52211). We chose the previously described constitutively active mutant (*49*) to maximize the chances of the enzyme being active in our system. The sequences for nanoLuc, GFP, mCherry, FGF2, and FGF4 were artificially synthesized using the codon optimization offered by the vendor. The phosphoinositide production enzymes were used with their native coding sequences except for PI4K in which we removed three translational pause sites specific to *E. coli* (*50*) and modified the 5′ end to eliminate potential loops in the RNA. These loops were identified with the RNAfold web server from the Institute for Theoretical Chemistry at the University of Vienna (*51*). These represent a total of 10 synonymous changes to the sequence of PI4K and are mostly in its N terminus.

Originally, we attempted to express all three enzymes required for phosphoinositide synthesis as an operon in the order required for synthesis but had problems detecting them by Western blot and thus modified the design to express PIS and PI4P5K as an operon in that order and PI4K separately. We performed the synonymous mutations to PI4K during this change to a dual promoter and, since the final construct proved successful, did not characterize the effects of the mutations or single promoter systematically. In all constructs, each of the enzymes was preceded by an N-terminal myc peptide tag (amino acid sequence EQKLISEEDL) and an optimized ribosome binding site (RBS) designed with the RBS calculator software to maximize their expression (*52*). Because the enzymes differ significantly in their size (~24, ~90, and ~60 kDa for PIS, PI4K, and PI4P5K, respectively), the use of the myc tag makes visualization of their expression in a single Western blot possible.

Bacterial strains and transformation procedures

For all cloning and plasmid maintenance procedures, we used the DH5α *E. coli* strain. While the system that we designed should work on

any *E. coli* strain, since it uses only the endogenous protein production machinery, we performed all the experiments using *E. coli* strain BL21 DE3, which is commonly used for protein overexpression owing to the presence of T7 polymerase (*53*). We chose this widely used strain to show that the production of phosphoinositides could be easily controlled in it, since it is most familiar to other researchers and thus the most likely strain to be used with our system in the future. Bacteria were made chemically competent in our laboratory using the Mix & Go *E. coli* Transformation Kit from Zymo Research, which follows a standard chemical competence protocol.

Culture conditions and bacterial characterization

Bacteria were grown in LB media supplemented with the appropriate antibiotics at 37°C for both plates and liquid cultures except for overnight cultures that were grown at 30°C to prevent the culture from reaching stationary phase. When small volumes of culture were needed, 6 ml was cultured in a 14-ml plastic tube. For larger cultures, we used Erlenmeyer flasks filled to 40% or less of their capacity to ensure proper aeration. Liquid cultures were grown in an orbital shaker at 260 rpm.

E. coli BL21 DE3 cells used for experiments were transformed with the appropriate plasmids, and a single colony was picked to grow overnight to an optical density at 600 nm (OD_{600}) between 0.8 and 3. The overnight culture OD_{600} was measured, and the appropriate amount of culture was diluted in fresh media with the appropriate concentration of inositol required for the experiment to reach an OD_{600} of 0.05. With the exception of the time course experiments, the bacteria were then grown for 3 hours or less after the dilution to guarantee that all measures were taken during the exponential growth phase, thus minimizing cell-to-cell variability.

The morphology of the cells carrying each of the constructs was inspected visually by spreading 1 μl of bacterial culture in a glass slide, which was then covered with a coverslip and imaged in a bright-field inverted microscope using a 60× water objective with a 1.5× objective in the light path and a 10× magnification eye/camera piece (900× total magnification). For the growth rate characterization of the cells carrying the different phosphoinositide production constructs, we used a 96-well plate format, loading 300 μl of the freshly diluted culture per well. The plate was incubated at 37°C, and OD_{600} was measured every 30 min. Four wells (replicates) were used for each measure, and a correction was performed for the increase in OD_{600} due to evaporation observed in the control well. This correction turned out to be unnecessary; the results do not vary noticeably if it is omitted. The slope of the linear approximation to the middle of the exponential phase of growth was measured in each replicate and averaged afterward among the four replicates for each experimental unit. Since the path length of the OD_{600} measure is not 1 cm as defined by convention, note that the value obtained does not correspond directly to those of OD_{600} measured routinely but should show a linear correspondence with such. Since, for our purposes, we only intend to show the lack of growth defects due to the constructs that we use, only the relative (not the absolute) levels are relevant.

For protein extractions, we pelleted the culture equivalent to 1 ml of culture at an OD_{600} of 1 and resuspended it in lysis buffer consisting of the BugBuster 10X Protein Extraction Reagent from Millipore, diluted to 1× final concentration, and supplemented with rLysozyme Solution and Benzonase Nuclease (purity, >90%; also from Millipore) according to the manufacturer's protocol. Protein gels were performed using the NuPAGE polyacrylamide system and transferred using the iBlot Dry Blotting System, both from Invitrogen, following the manufacturer's protocols. The membrane was then probed with the horseradish peroxidase–labeled 9E10 monoclonal antibody against the myc tag obtained from OriGene (then Acris Antibodies). Western blots were imaged using the C-DiGit Chemiluminescence Western Blot Scanner and the WesternSure Chemiluminescent Substrate from LI-COR according to the manufacturer's protocol.

Lipid extraction, quantification, and characterization

For lipid extraction, a volume of culture equivalent to 10 ml of OD_{600} 1.0 was pelleted, and phospholipids were extracted using a variant of the Bligh-Dyer protocol (*54*). Briefly, the pellet was resuspended in 420 μl of water, and 1250 μl of methanol and 625 μl of chloroform were added in that order. This mix was vortexed, and another 625 μl of chloroform was added. After vortexing of the new mix, 600 μl of water was added and the mix was vortexed again. Last, 25 μl of HCl was added to acidify the mix, and after repeat vortexing, the mix was centrifuged at 150 rcf for 5 min. The bottom (organic) phase was then dried under argon and resuspended in a chloroform/methanol 20:9 mix. The extracted lipids were then stored at −20°C until measurements were carried out, 1 to 10 days after the extraction. PI4P and PIP2 abundances were measured using a competitive ELISA commercially available from Echelon Biosciences. On the day of the ELISA tests, an aliquot of 6 μl or less of the extracted lipids was dried and resuspended according to the ELISA protocol. A minor level of signal is always detected in these ELISA tests, even for controls, indicating some background level of noise when using phospholipids extracted from *E. coli*. These ELISAs proved to be problematic, in many cases showing only a background signal for all samples. Repeating the ELISA test on a different day with the same extracts and protocol was the only way to successfully measure the phosphoinositides. We therefore only report data from tests in which the samples show variation depending on the construct used; this means that unsuccessful ELISA tests, for which no signal was detected above background for any samples, were not used. While this could potentially introduce a sampling bias by selecting only for positive results, the samples measured successfully are the same as those that produced no signal on the failed test days; thus, there is no risk of bias in the results reported. Troubleshooting the assay with the vendor's suggestions did not help; the presumption is that differences in room temperature and/or humidity alter the first step of the ELISA process in which the phospholipids are resuspended in an aqueous solution; thus, in failed tests, the presumption is that the lipid never resuspended successfully. The test is reported by the vendor to be robust, and it is possible that the shorter lipid tails produced in bacteria are responsible for this erratic behavior. Initially, we used a strip lipid protein overlay for PI4P detection (also from Echelon Biosciences), which worked reliably, but this product was discontinued and we could not reproduce its signal-to-noise ratios even when acquiring all the reagents from the same company.

To characterize the phosphoinositides produced in the bacteria, we used Avanti Polar Lipids' analytical services to get a first view of the different phospholipid classes. For this analysis, we sent dry lipid extracts processed as described earlier and dried under argon. At the vendor's facilities, the lipids were re-extracted to remove impurities, and this extract was then analyzed by mass spectrometry with the appropriate standards for quantification. This analysis, however, was only performed for PI, since phosphorylated phosphoinositides are not easily modified to be amenable for mass spectrometry. We also

used the services of ATK Innovation, Analytics and Discovery (North Bend, WA), which performed a comprehensive mass spectrometry analysis of our samples. Phosphoinositides were measured in acidic extracts both with and without prior neutral extraction using a chemical modification of the phosphate group in the phosphorylated phosphoinositides as described in the literature (*55*, *56*). Neutral lipids were measured using methods adapted from those of Hines *et al.* (*57*). Internal standards obtained from Avanti Polar Lipids (Alabaster, AL) added at the beginning of the extraction protocol paired with standard curves in comparable samples were used to normalize data, controlling for extraction bias and matrix effects. We used the data obtained with this quantification to perform a linear conversion on the ELISA data to correct for extraction and protocol losses.

Endogenous phosphatase tests

As a first approach, to test whether endogenous phosphatases from *E. coli* are the cause of the relatively low phosphorylated phosphoinositide abundance relative to the PI abundance, we performed a kinase inhibitor test. For this test, we grew the bacteria in media with 5 mM inositol to the previously determined plateau in phosphoinositide production (3 hours) and split the culture into treatment and control, adding a kinase inhibitor for the treatment and growing the cells for one more hour before harvesting and measuring the phosphoinositides by mass spectrometry. We used PIK-93 from Selleckchem at 1 μM final concentration to inhibit PI4K (*58*) and ISA-2011B from MedChemExpress at 20 μM final concentration to inhibit PI4P5K (*59*).

Phosphoinositide localization tests

To create the PLCδ-PH domain non–PIP2-binding mutant, we performed nonsynonymous mutations, substituting eight amino acids for alanine, such that the interaction would be impaired. Following the numbering of Ferguson and coworkers (*39*), whose paper we used to guide these mutations, the changes made were K30A, K32A, W36A, R40A, E54A, S55A, R56A, and K57A.

The cells for these experiments were visualized using a LEICA scanning confocal microscope with the pinhole aperture set at 1 Airy unit relative to the fluorescence of GFP at 507 nm (1 Airy = 128 μm). Excitation was done sequentially with a laser set at 488 and 587 nm for GFP and mCherry, respectively, and with acquisition on the range of 500 to 570 nm for GFP and 600 to 670 nm for mCherry. A 100× HC PL APO oil objective of numerical aperture 1.44 was used. To improve the speed of the measurement and minimize photobleaching, only a fraction of the image was scanned, a square of side 29 μm at a resolution of 512 × 512 pixels, which was scanned at 100 Hz.

To provide a quantitative measure of the change in localization of the reporter, we devised an index based on a line scan perpendicular to the major axis of the cell performed with the ImageJ software (*60*). This line is done on the center of the cell, to avoid the cell poles, where inclusion bodies can form, thus avoiding a confounding factor that could erroneously be interpreted as membrane localization if analyzing only the line. The expectation is then that, for the control channel (in red since it is given by mCherry), the line scan should show a unimodal distribution. For the reporter channel (in green), two different behaviors are expected: The line scan should also show a unimodal distribution overlapping with the red channel in the control experiments, but in the cells with the detected phosphoinositide, it should have a bimodal distribution with a dip in the middle. This behavior can be seen in Fig. 5A.

To minimize noise in the line scan analysis, we used a 10-pixel-thick line, such that random noise would be averaged. The lines were drawn manually on the red control channel such that there could be no experimental bias in the selection of the cells. The line scan was then standardized to its maximum so that variation is between 0 and 1, and differences in the levels of fluorescence between cells or channels did not affect the calculations. The first part of the index was then calculated for the green channel by splitting the line scan into three regions, the central 0.5 μm as the center region and the remainder of the line on each side as the left or right side accordingly. The scans were aligned manually. Once the line scan is performed, the maximum of the left side and that of the right side were averaged and divided by the minimum in the center region. For a curve that follows a normal or symmetric unimodal distribution, the maximum outside of the center area should be basically the same as the minimum inside, giving a value close to 1. On the other hand, if the curve is bimodal, then the value should be higher than 1 because the average of the maximums outside the center area should be higher than the minimum inside (where the dip occurs).

While the scan of the green channel would be enough to detect the change of the reporter localization, the alignment of the line scans when defining the center region could introduce noise into the calculations because errors in the alignment would cause the average of the outside regions to be higher than the minimum in the center region. While errors of alignment should be small, the index can be improved by also using the red control channel. The final index is the value for the green channel (first part of the index) divided by the red channel (second part of the index). In this way, any error caused by misalignment is corrected since the value for both green and red channels would show the same bias, thus taking the index back to 1 should both curves coincide. Figure S3 shows a schematic of the calculation of the index.

To obtain the distribution of the bimodality index for each population of cells, we scored 10 cells per field in four different fields for each experimental condition. As described earlier, the cells were chosen blindly in the red channel, and the only consideration for the selection was for the cell to be separate enough from other cells such that the line scan would reach the background level at its extremes, as opposed to rising again by going into a different cell. The values obtained in this way were then used to calculate a one-way ANOVA and a post hoc Tukey HSD test.

FGF2 and FGF4 export assay

To assay export of FGF2, we expressed a small luciferase, nanoLuc, at its C terminus. The nanoLuc substrate is not membrane permeable; thus, signal should be greatly increased upon export of the FGF2-nanoLuc fusion protein to the outside of the plasma membrane. We performed these experiments on several mutants that should diminish or enhance the export of FGF2 and of FGF4 (see Results).

For these experiments, cells were grown in tubes containing variable amounts of inositol for 3 hours, after which 50 μl of culture was pipetted to a well of a 96-well plate. This was diluted with 30 μl of freshly made phosphate-buffered saline (PBS; pH 7.0) containing 30 μl of substrate for nanoLuc (N113A, Promega) per 10 ml of buffer. At this point, OD_{600} and luminescence were measured on a plate reader giving the background level of luminescence for each treatment. Notably, because of the dilution and the different path length, this would not be the OD_{600} as it would be standardly measured in the culture, but simply a linear function of OD_{600}, useful to identify gross errors in pipetting

and to verify lysis after the addition of lysis buffer. After the measure of the background luminescence, or prelysis luminescence, we added 100 µl of PBS (pH 7.0) with BugBuster such that the final concentration of BugBuster in the mix would be 1×. Lysis was allowed to run for 15 min and confirmed by the decrease of the OD_{600} reading in the well. After lysis was confirmed, 20 µl of freshly made PBS (pH 7.0) containing 20 µl of substrate per 10 ml of buffer was added to each well and luminescence was measured again, resulting in the postlysis measurement. All measures were performed immediately after substrate addition to guarantee substrate excess and the validity of the measurement. The pre- and postlysis measures are not directly equivalent since the enzyme is in a different environment for each case. Thus, the usefulness of the measurement is not in its absolute value but in the pattern of the values observed for the different constructs.

For the analysis, we used an index created by dividing the value of prelysis luminescence times 100 over the postlysis luminescence. This can be viewed as a percentage of total luminescence present before lysis. Note that if the activity of the nanoLuc is different in the cytosol compared to the media used for lysis, this is may not reflect an absolute fraction of luminescence in the cytosol. However, since we used the same external buffer in all experiments, it does reflect the relative levels of cytosolic luminescence between different experiments. The values obtained in this way were then used to calculate a three-way ANOVA and a post hoc Tukey HSD test.

SUPPLEMENTARY MATERIALS

Supplementary material for this article is available at http://advances.sciencemag.org/cgi/content/full/5/3/eaat4872/DC1

Fig. S1. Abnormal morphology observed.
Fig. S2. Detection of PI4P.
Fig. S3. Calculation of the bimodality index.
Fig. S4. Representative images for the bimodality tests.
Fig. S5. Pilot experiment on FGF2 export.
Fig. S6. FGF2 export depending on the phosphoinositides present.
Table S1. Lipid species detected.

REFERENCES AND NOTES

1. Y. Koga, H. Morii, Biosynthesis of ether-type polar lipids in archaea and evolutionary considerations. *Microbiol. Mol. Biol. Rev.* **71**, 97–120 (2007).
2. T. G. Kutateladze, Translation of the phosphoinositide code by PI effectors. *Nat. Chem. Biol.* **6**, 507–513 (2010).
3. C. Cauvin, A. Echard, Phosphoinositides: Lipids with informative heads and mastermind functions in cell division. *Biochim. Biophys. Acta* **1851**, 832–843 (2015).
4. K. Tsujita, T. Itoh, Phosphoinositides in the regulation of actin cortex and cell migration. *Biochim. Biophys. Acta* **1851**, 824–831 (2015).
5. S. Suetsugu, S. Kurisu, T. Takenawa, Dynamic shaping of cellular membranes by phospholipids and membrane-deforming proteins. *Physiol. Rev.* **94**, 1219–1248 (2014).
6. L. Chen, Q. Zhang, Y. Qiu, Z. Li, Z. Chen, H. Jiang, Y. Li, H. Yang, Migration of PIP_2 lipids on voltage-gated potassium channel surface influences channel deactivation. *Sci. Rep.* **5**, 15079 (2015).
7. J. P. Steringer, S. Bleicken, H. Andreas, S. Zacherl, M. Laussmann, K. Temmerman, F. X. Contreras, T. A. M. Bharat, J. Lechner, H.-M. Müller, J. A. G. Briggs, A. J. García-Sáez, W. Nickel, Phosphatidylinositol 4,5-bisphosphate ($PI(4,5)P_2$)-dependent oligomerization of fibroblast growth factor 2 (FGF2) triggers the formation of a lipidic membrane pore implicated in unconventional secretion. *J. Biol. Chem.* **287**, 27659–27669 (2012).
8. R. Fiume, Y. Stijf-Bultsma, Z. H. Shah, W. jan Keune, D. R. Jones, J. Jude, N. Divecha, PIP4K and the role of nuclear phosphoinositides in tumour suppression. *Biochim. Biophys. Acta* **1851**, 898–910 (2015).
9. M. Pittet, A. Conzelmann, Biosynthesis and function of GPI proteins in the yeast *Saccharomyces cerevisiae*. *Biochim. Biophys. Acta* **1771**, 405–420 (2007).
10. Y. Nishizuka, Intracellular signaling by hydrolysis of phospholipids and activation of protein kinase C. *Science* **258**, 607–614 (1992).
11. S. Jean, A. A. Kiger, Coordination between RAB GTPase and phosphoinositide regulation and functions. *Nat. Rev. Mol. Cell Biol.* **13**, 463–470 (2012).
12. T. Balla, Inositol-lipid binding motifs: Signal integrators through protein-lipid and protein-protein interactions. *J. Cell Sci.* **118**, 2093–2104 (2005).
13. S. Mukhopadhyay, P. K. Jackson, The tubby family proteins. *Genome Biol.* **12**, 225 (2011).
14. J. M. Kavran, D. E. Klein, A. Lee, M. Falasca, S. J. Isakoff, E. Y. Skolnik, M. A. Lemmon, Specificity and promiscuity in phosphoinositide binding by pleckstrin homology domains. *J. Biol. Chem.* **273**, 30497–30508 (1998).
15. M. J. Berridge, R. F. Irvine, Inositol trisphosphate, a novel second messenger in cellular signal transduction. *Nature* **312**, 315–321 (1984).
16. N. Borges, L. G. Gonçalves, M. V. Rodrigues, F. Siopa, R. Ventura, C. Maycock, P. Lamosa, H. Santos, Biosynthetic pathways of inositol and glycerol phosphodiesters used by the hyperthermophile *Archaeoglobus fulgidus* in stress adaptation. *J. Bacteriol.* **188**, 8128–8135 (2006).
17. M. R. Macbeth, H. L. Schubert, A. P. VanDemark, A. T. Lingam, C. P. Hill, B. L. Bass, Inositol hexakisphosphate is bound in the ADAR2 core and required for RNA editing. *Science* **309**, 1534–1539 (2005).
18. A. Saiardi, R. Bhandari, A. C. Resnick, A. M. Snowman, S. H. Snyder, Phosphorylation of proteins by inositol pyrophosphates. *Science* **306**, 2101–2105 (2004).
19. B. Antonsson, Phosphatidylinositol synthase from mammalian tissues. *Biochim. Biophys. Acta* **1348**, 179–186 (1997).
20. Y. Liu, V. A. Bankaitis, Phosphoinositide phosphatases in cell biology and disease. *Prog. Lipid Res.* **49**, 201–217 (2010).
21. R. A. Anderson, I. V. Boronenkov, S. D. Doughman, J. Kunz, J. C. Loijens, Phosphatidylinositol phosphate kinases, a multifaceted family of signaling enzymes. *J. Biol. Chem.* **274**, 9907–9910 (1999).
22. M. A. De Matteis, C. Wilson, G. D'Angelo, Phosphatidylinositol-4-phosphate: The Golgi and beyond. *Bioessays* **35**, 612–622 (2013).
23. A. Gambhir, G. Hangyás-Mihályné, I. Zaitseva, D. S. Cafiso, J. Wang, D. Murray, S. N. Pentyala, S. O. Smith, S. McLaughlin, Electrostatic sequestration of PIP_2 on phospholipid membranes by basic/aromatic regions of proteins. *Biophys. J.* **86**, 2188–2207 (2004).
24. G. R. V. Hammond, T. Balla, Polyphosphoinositide binding domains: Key to inositol lipid biology. *Biochim. Biophys. Acta* **1851**, 746–758 (2015).
25. J. Viaud, R. Mansour, A. Antkowiak, A. Mujalli, C. Valet, G. Chicanne, J.-M. Xuereb, A.-D. Terrisse, S. Séverin, M.-P. Gratacap, F. Gaits-Iacovoni, B. Payrastre, Phosphoinositides: Important lipids in the coordination of cell dynamics. *Biochimie* **125**, 250–258 (2016).
26. A. Das-Chatterjee, L. Goswami, S. Maitra, K. G. Dastidar, S. Ray, A. L. Majumder, Introgression of a novel salt-tolerant L-*myo*-inositol 1-phosphate synthase from *Porteresia coarctata* (Roxb.) Tateoka (*PcINO1*) confers salt tolerance to evolutionary diverse organisms. *FEBS Lett.* **580**, 3980–3988 (2006).
27. K. L. Martin, T. K. Smith, Phosphatidylinositol synthesis is essential in bloodstream form *Trypanosoma brucei*. *Biochem. J.* **396**, 287–295 (2006).
28. S. M. Simon, G. Blobel, A protein-conducting channel in the endoplasmic reticulum. *Cell* **65**, 371–380 (1991).
29. W. Nickel, The unconventional secretory machinery of fibroblast growth factor 2. *Traffic* **12**, 799–805 (2011).
30. A. D. Ebert, M. Laußmann, S. Wegehingel, L. Kaderali, H. Erfle, J. Reichert, J. Lechner, H.-D. Beer, R. Pepperkok, W. Nickel, Tec-kinase-mediated phosphorylation of fibroblast growth factor 2 is essential for unconventional secretion. *Traffic* **11**, 813–826 (2010).
31. K. Temmerman, W. Nickel, A novel flow cytometric assay to quantify interactions between proteins and membrane lipids. *J. Lipid Res.* **50**, 1245–1254 (2009).
32. K. Temmerman, A. D. Ebert, H.-M. Müller, I. Sinning, I. Tews, W. Nickel, A direct role for phosphatidylinositol-4,5-bisphosphate in unconventional secretion of fibroblast growth factor 2. *Traffic* **9**, 1204–1217 (2008).
33. L. C. Torrado, K. Temmerman, H.-M. Müller, M. P. Mayer, C. Seelenmeyer, R. Backhaus, W. Nickel, An intrinsic quality-control mechanism ensures unconventional secretion of fibroblast growth factor 2 in a folded conformation. *J. Cell Sci.* **122**, 3322–3329 (2009).
34. H.-M. Müller, J. P. Steringer, S. Wegehingel, S. Bleicken, M. Münster, E. Dimou, S. Unger, G. Weidmann, H. Andreas, A. J. García-Sáez, K. Wild, I. Sinning, W. Nickel, Formation of disulfide bridges drives oligomerization, membrane pore formation, and translocation of fibroblast growth factor 2 to cell surfaces. *J. Biol. Chem.* **290**, 8925–8937 (2015).
35. D. Oursel, C. Loutelier-Bourhis, N. Orange, S. Chevalier, V. Norris, C. M. Lange, Lipid composition of membranes of *Escherichia coli* by liquid chromatography/tandem mass spectrometry using negative electrospray ionization. *Rapid Commun. Mass Spectrom.* **21**, 1721–1728 (2007).
36. A. Balla, G. Tuymetova, A. Tsiomenko, P. Várnai, T. Balla, A plasma membrane pool of phosphatidylinositol 4-phosphate is generated by phosphatidylinositol 4-kinase type-III alpha: Studies with the PH domains of the oxysterol binding protein and FAPP1. *Mol. Biol. Cell* **16**, 1282–1295 (2005).
37. G. R. V. Hammond, M. P. Machner, T. Balla, A novel probe for phosphatidylinositol 4-phosphate reveals multiple pools beyond the Golgi. *J. Cell Biol.* **205**, 113–126 (2014).

38. S. A. Watt, G. Kular, I. N. Fleming, C. P. Downes, J. M. Lucocq, Subcellular localization of phosphatidylinositol 4,5-bisphosphate using the pleckstrin homology domain of phospholipase C δ1. *Biochem. J.* **363**, 657–666 (2002).
39. K. M. Ferguson, M. A. Lemmon, J. Schlessinger, P. B. Sigler, Structure of the high affinity complex of inositol trisphosphate with a phospholipase C pleckstrin homology domain. *Cell* **83**, 1037–1046 (1995).
40. N. H. Tolia, L. Joshua-Tor, Strategies for protein coexpression in *Escherichia coli*. *Nat. Methods* **3**, 55–64 (2006).
41. J. H. Davis, A. J. Rubin, R. T. Sauer, Design, construction and characterization of a set of insulated bacterial promoters. *Nucleic Acids Res.* **39**, 1131–1141 (2011).
42. C. R. H. Raetz, Phosphatidylserine synthetase mutants of *Escherichia coli*. Genetic mapping and membrane phospholipid composition. *J. Biol. Chem.* **251**, 3242–3249 (1976).
43. W. Xia, W. Dowhan, Phosphatidylinositol cannot substitute for phosphatidylglycerol in supporting cell growth of *Escherichia coli*. *J. Bacteriol.* **177**, 2926–2928 (1995).
44. M. R. Wenk, L. Lucast, G. di Paolo, A. J. Romanelli, S. F. Suchy, R. L. Nussbaum, G. W. Cline, G. I. Shulman, W. McMurray, P. de Camilli, Phosphoinositide profiling in complex lipid mixtures using electrospray ionization mass spectrometry. *Nat. Biotechnol.* **21**, 813–817 (2003).
45. S. McLaughlin, J. Wang, A. Gambhir, D. Murray, PIP_2 and proteins: Interactions, organization, and information flow. *Annu. Rev. Biophys. Biomol. Struct.* **31**, 151–175 (2002).
46. A. K. Bose, K. A. Janes, A high-throughput assay for phosphoprotein-specific phosphatase activity in cellular extracts. *Mol. Cell. Proteomics* **12**, 797–806 (2013).
47. J. C. Loijens, R. A. Anderson, Type I phosphatidylinositol-4-phosphate 5-kinases are distinct members of this novel lipid kinase family. *J. Biol. Chem.* **271**, 32937–32943 (1996).
48. X.-H. Zhao, T. Bondeva, T. Balla, Characterization of recombinant phosphatidylinositol 4-kinase β reveals auto- and heterophosphorylation of the enzyme. *J. Biol. Chem.* **275**, 14642–14648 (2000).
49. S. Kang, A. G. Bader, P. K. Vogt, Phosphatidylinositol 3-kinase mutations identified in human cancer are oncogenic. *Proc. Natl. Acad. Sci. U.S.A.* **102**, 802–807 (2005).
50. M. H. Larson, R. A. Mooney, J. M. Peters, T. Windgassen, D. Nayak, C. A. Gross, S. M. Block, W. J. Greenleaf, R. Landick, J. S. Weissman, A pause sequence enriched at translation start sites drives transcription dynamics in vivo. *Science* **344**, 1042–1047 (2014).
51. A. R. Gruber, R. Lorenz, S. H. Bernhart, R. Neuböck, I. L. Hofacker, The Vienna RNA Websuite. *Nucleic Acids Res.* **36**, W70–W74 (2008).
52. A. Espah Borujeni, A. S. Channarasappa, H. M. Salis, Translation rate is controlled by coupled trade-offs between site accessibility, selective RNA unfolding and sliding at upstream standby sites. *Nucleic Acids Res.* **42**, 2646–2659 (2014).
53. F. W. Studier, B. A. Moffatt, Use of bacteriophage T7 RNA polymerase to direct selective high-level expression of cloned genes. *J. Mol. Biol.* **189**, 113–130 (1986).
54. E. G. Bligh, W. J. Dyer, A rapid method of total lipid extraction and purification. *Can. J. Biochem. Physiol.* **37**, 911–917 (1959).
55. A. Traynor-Kaplan, M. Kruse, E. J. Dickson, G. Dai, O. Vivas, H. Yu, D. Whittington, B. Hille, Fatty-acyl chain profiles of cellular phosphoinositides. *Biochim. Biophys. Acta* **1862**, 513–522 (2017).
56. A. Kielkowska, I. Niewczas, K. E. Anderson, T. N. Durrant, J. Clark, L. R. Stephens, P. T. Hawkins, A new approach to measuring phosphoinositides in cells by mass spectrometry. *Adv. Biol. Regul.* **54**, 131–141 (2014).
57. K. M. Hines, A. Waalkes, K. Penewit, E. A. Holmes, S. J. Salipante, B. J. Werth, L. Xu, Characterization of the mechanisms of daptomycin resistance among Gram-positive bacterial pathogens by multidimensional lipidomics. *mSphere* **2**, e00492-17 (2017).
58. R. Dooley, E. Angibaud, Y. R. Yusef, W. Thomas, B. J. Harvey, Aldosterone-induced ENaC and basal Na^+/K^+-ATPase trafficking via protein kinase D1-phosphatidylinositol 4-kinaseIIIβ trans Golgi signalling in M1 cortical collecting duct cells. *Mol. Cell. Endocrinol.* **372**, 86–95 (2013).
59. J. Semenas, A. Hedblom, R. R. Miftakhova, M. Sarwar, R. Larsson, L. Shcherbina, M. E. Johansson, P. Härkönen, O. Sterner, J. L. Persson, The role of PI3K/AKT-related PIP5K1α and the discovery of its selective inhibitor for treatment of advanced prostate cancer. *Proc. Natl. Acad. Sci. U.S.A.* **111**, E3689–E3698 (2014).
60. C. A. Schneider, W. S. Rasband, K. W. Eliceiri, NIH image to ImageJ: 25 years of image analysis. *Nat. Methods* **9**, 671–675 (2012).

Acknowledgments: We thank A. Smogorzewska, B. Chait, and A. K. Menon for their role as advisers during S.B.'s PhD thesis project. We also thank S. Honerkamp-Smith for work in editing and composing all figures for the paper and two anonymous reviewers who suggested experiments to improve the paper. **Funding:** This project was funded by The Rockefeller University. S.M.S. was partially supported by NIH 1P50CA210964 and 5R56CA207929. **Author contributions:** S.B. and S.M.S. conceived the project and designed the experimental approach. S.B. and R.C.-C. conducted the experiments and troubleshot them. S.B. wrote the first draft with all authors editing it and approving the paper. **Competing interests:** The authors declare that they have no competing interests. **Data and materials availability:** All data are presented in the paper and the plasmids used in this study have been deposited on the Addgene database. Additional data related to this paper may be requested from the authors.

Submitted 3 March 2018
Accepted 4 February 2019
Published 27 March 2019
10.1126/sciadv.aat4872

Citation: S. Botero, R. Chiaroni-Clarke, S. M. Simon, *Escherichia coli* as a platform for the study of phosphoinositide biology. *Sci. Adv.* **5**, eaat4872 (2019).

Escherichia coli as a platform for the study of phosphoinositide biology

Sergio Botero, Rachel Chiaroni-Clarke and Sanford M. Simon

Sci Adv **5** (3), eaat4872.
DOI: 10.1126/sciadv.aat4872